Chapter 7

Finite element simulation of multiaxial forging for Fe-30Mn-9Al-0.8C low-density steel using microstructure based modified Johnson-Cook constitutive equation

7.1 Introduction

It is observed in chapter 6 that the role of dislocation density in strengthening the material is significant compared to grain refinement. This investigation seeks to establish a theoretical correlation between these observed microstructural phenomena and the equivalent strain experienced by the material during MAF. The identified relations have been integrated into our previously formulated J-C model to precisely capture the flow stress characteristics. A modified J-C model with the effect of dislocation density and grain size has been formulated to predict the flow stress and the strength of material achieved after each MAF pass. Thereafter, FE analysis has been carried out to replicate the actual microstructural evolution during the MAF process. To emphasize the role of strengthening parameters in predicting the flow stress in every MAF pass accurately, a material VUMAT subroutine in ABAQUS has been created for a modified J-C constitutive model that accounts for the role of increased dislocation density and grain size.

7.2 Results and discussion

7. 2.1 Modified J-C constitutive model

As indicated in the objectives, accurate reproduction of the material response following each MAF pass is crucial because the deformation behavior depends on the loading conditions and the history of deformation in the material. As observed in chapter 6 that a significant deformation occurs at 250 ℃ and at moderate strain rate. Due to the complexity of the deformation condition, the material exhibits strain hardening with a non-linear

deformation behavior in the material. However, strain accumulation occurs with microstructural evolution after every MAF pass and consequently there is an increase in the yield strength. The major contribution of the yield strength comes from the grain boundary strengthening ($\Delta\sigma_g$), dislocation strengthening ($\Delta\sigma_\rho$) and other strengthening of either precipitate or solid solution ($\Delta\sigma_{others}$) and therefore the modified equation of yield stress can be written as

$$\sigma_y = \sigma_0 + \Delta\sigma_g + \Delta\sigma_\rho + \Delta\sigma_{others} \quad (18)$$

At MAF-0, all the strengthening parameters are already included in σ_0. But in further MAF passes, they have a significant role in increasing the YS. The precipitate strengthening comes from the precipitates forming during the cooling and solidification of a material. Since the steel composition is unaltered in the current experimental setting, the solid solution strengthening contribution can be viewed as the same for all samples. Since there is no difference between the carbides before and after the MAF pass, as illustrated by the X-ray patterns in Fig. 34a, the precipitation enhancement brought on by carbides may likewise be considered constant. A reduction in grain size (d) in subsequent MAF passes is observed in Fig. 32, thereby strengthens the material. The contribution of the refined grains to the strength is described directly by the Hall-Petch relationship [196-197] as

$$\Delta\sigma_g = k\,({g_f}^{-1/2} - {g_0}^{-1/2}) \quad (19)$$

Where, k is a material constant, g_0 is initial grain size and g_f is grain size during MAF. Eq. (19) shows the relationship between yield strength and grain size for a range of grain sizes (50-13 μm) with MAF pass in steels. With each additional MAF pass, grain boundary strengthening results in an increase in yield strength, that's how k is calculated as 2374 MPa [53].

The contribution of dislocation to yield strength is estimated by the Taylor equation [183] as

$$\Delta\sigma_\rho = \alpha MGb(\rho_f^{1/2} - \rho_0^{1/2})$$

(20)

Where, ρ_0 is the initial dislocation density, ρ_f is the dislocation density during MAF, α is the Taylor constant with a value of 0.24, M is the average Taylor factor with a value of 3.0, [198-199] and G is the shear modulus which is equal to 61 GPa.

As discussed above, the complex strengthening relation on the flow stress is not reflected by the original J-C model and hence, considering the influence of each strengthening parameter to yield strength after each MAF pass, the original J-C can be modified in the present context as follows:

$$\sigma_{flow} = \left(\sigma_0 + k\,(g_f^{\frac{-1}{2}} - g_0^{\frac{-1}{2}}) + \alpha MGb((\rho_f^{\frac{1}{2}} - \rho_0^{\frac{1}{2}}) + B\varepsilon^n\right)\left[1 + Cln\left(\frac{\dot{\varepsilon}}{\dot{\varepsilon}_0}\right)\right]\ \left[1 - \left(\frac{T-T_r}{T_m-T_r}\right)^m\right]$$

(21)

7.*2.2* Dependency of dislocation density on strain

Odnobokova et al. [200] have examined the impact of cold rolling and multidirectional forging over 316L. They have reported that the dislocation density rises from 2 x 10^{15} m^{-2} to 4 x 10^{15} m^{-2} for cold rolling and from 6 x 10^{15} m^{-2} to 7.5 x 10^{15} m^{-2} for multidirectional forging when the total strain value is 4. Thus, a trend of increase in dislocation densities with the plastic strain is observed in cold working processes. Singh et. al. [185] have proposed an empirical relation (Eq. (22)) to calculate the increase in dislocation density with the imposed equivalent strain imparted during the constrained grooves pressing at warm conditions.

$$\rho_f = \rho_0 + k_1(1 - \exp(-k_2\varepsilon))$$

(22)

Where, ρ_0 is the dislocation density of initial material, ε is the imposed equivalent plastic strain. Further, k_1 and k_2 are the constants obtained from the non-linear curve fit of

experimental dislocation density and imposed strain estimated in [67], [181] for cold rolling. The same relation is used in the present investigation where ρ_0 is dislocation density of MAF-0. The constants k_1 and k_2 are obtained by curve fitting of dislocation density vs imposed equivalent strain (data from Table 11). The fitting curve (Fig. 40) for experimental material finds k_1 to be 7.9 x 1015 m^{-2} and k_2 to be -1.813.

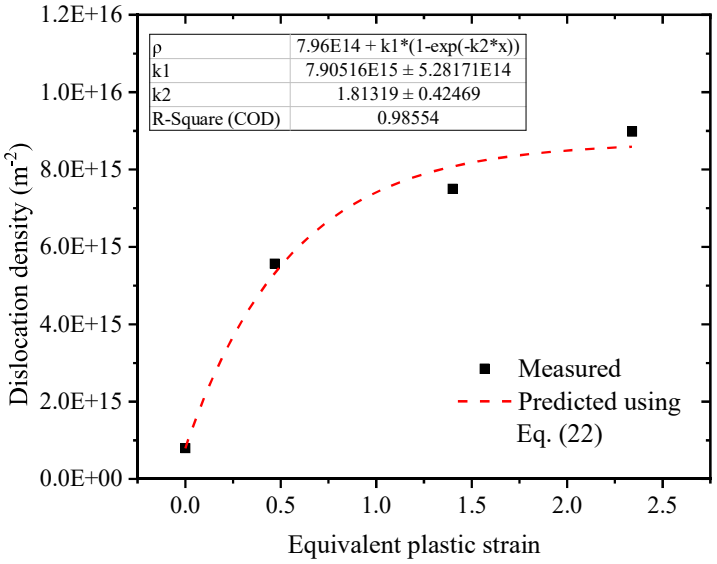

Fig. 40: Effect of equivalent plastic strain on dislocation density.

With increase in amount of imposed plastic strain, initially dislocation density increases, reaching to a maximum, and thereafter it remains almost constant. Therefore, dislocations are rearranging at a critical strain 2.3 or five passes of MAF.

7.*2.3* Dependency of grain size on strain

One can observe changes in the distribution of grain sizes with an increasing number of deformations passes (Fig. 41a). The solutionised and quenched material has grains of average size of 50 µm (data is also verified from measurement from optical microstructure). The initial grain size distribution was relatively wide, but as deformation progressed, the

distribution became narrower and more uniform for 5th passes. During the MAF process, the initial grain size of austenite undergoes a significant reduction, reaching 35 μm and 20 μm after first and third pass, respectively. Subsequently, as the MAF pass continues up to five passes to a total strain of 2.3, there is a further gradual reduction in the grain size, ultimately reaching approximately 13 μm. This is due to uniform compression from all three directions. This indicates that the forging process effectively breaks down larger grains into smaller ones, leading to the development of lamellar grains with a transverse dimension of about 13 μm. In regions with a high degree of strain concentration or deformation gradients, there are variations in the grain size. As the number of deformations passes increases, there is refinement in the grain size. The plastic deformation introduced during forging promotes grain subdivision and reduces the average grain size. This means grain boundaries become more intricate, and the individual grain becomes discretized. It has been suggested in [43] that the grain size (g_f) during cold rolling can be expressed by an exponential function of equivalent plastic strain as

$$g_f = g_0 \exp(-k_3 \varepsilon) \quad (23)$$

Where, ε is the imposed equivalent strain, g_0 is initial grain size and k_3 is strengthening constant. In the present investigation, Eq. (23) is fitted with the plot (Fig. 41b) of imposed equivalent strain and the grain size of multiaxially forged samples and k_3 is found to be 0.639.

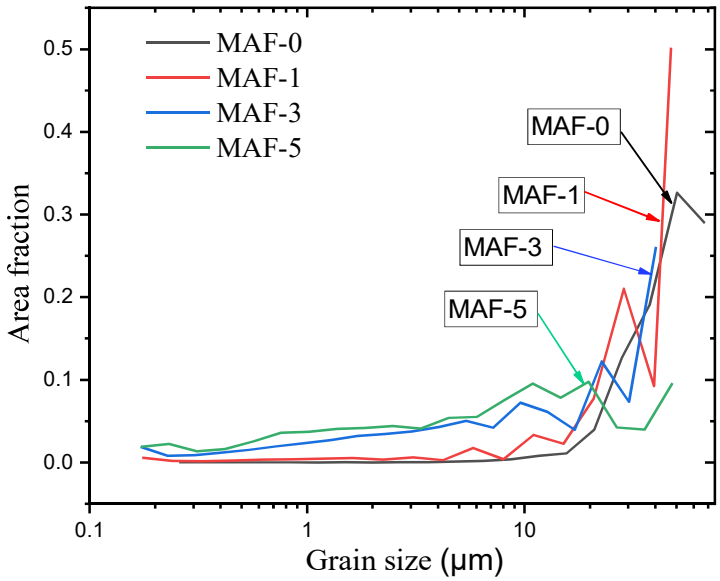

(a)

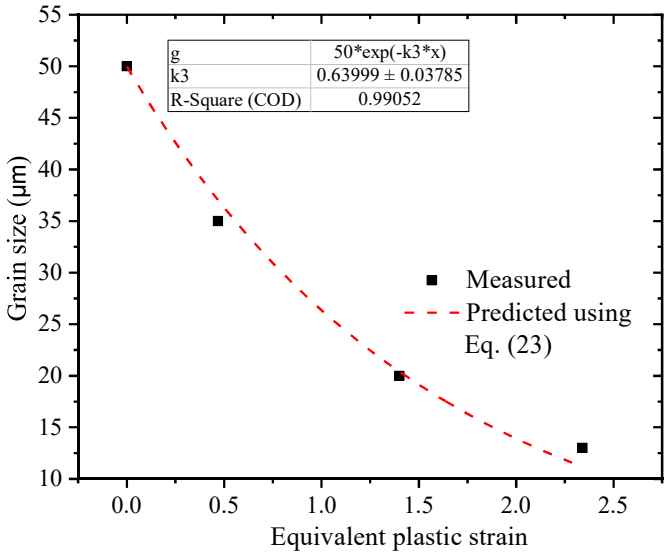

(b)

Fig. 41: (a) Plots of area fraction against grain size, (b) Effect of equivalent plastic strain on grain size.

7.2.4 Finite element analysis of multiaxial forging

A 3-D finite element model of a rectangular sample is created with the J-C constitutive model to explore the consequence of dislocation density increment and grain size reduction during the MAF process. To include the modified J-C constitutive equation, i. e. Eq. (21) into the FE model, a VUMAT subroutine in ABAQUS for Fe-30Mn-9Al-0.8C steel is first constructed. Figure 42 shows the flow chart of the developed VUMAT subroutine. The implemented user subroutine uses six state-dependent variables (SDVs), as shown in Table 15. The original J-C model parameters of the current material have been evaluated in chapter 5. The material properties of the current material are summarized in Table 16. To provide a concise overview of the numerical simulation results for the MAF of the blank, experimental results of MAF-1, MAF-3, and MAF-5 have been considered for comparison.

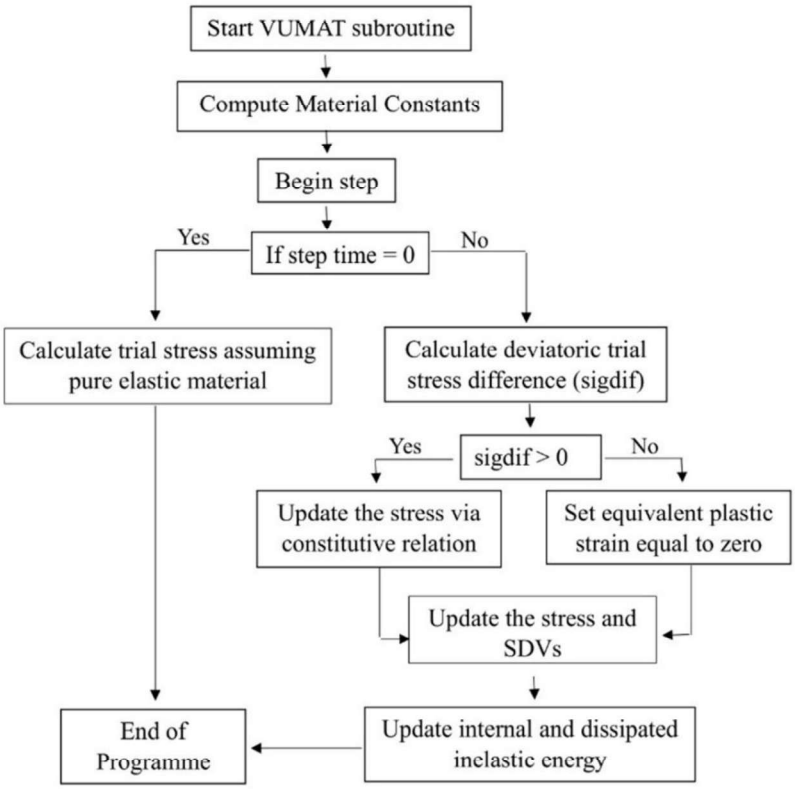

Fig. 42: Flow chart for VUMAT.

Table 15: VUMAT state-dependent variable definition and allocation.

Variable name	**VUMAT allocation**
Equivalent plastic strain (ε_p^n)	SDV1
Equivalent plastic strain rate ($\dot{\varepsilon}_p^n$)	SDV2
Dislocation density (ρ_f)	SDV3
Flow stress (σ_{flow})	SDV4
Yield strength (σ_y)	SDV5
Grain size (g_f)	SDV6

Table 16: Material properties of Fe-30Mn-9Al-0.8C low-density steel.

Material Properties	**Values**
Density (gm/cm^3)	6.8
Young's modulus (MPa)	160000
Poisson's ratio	0.3
σ_0 (MPa)	380
B (MPa)	1860
Dislocation strengthening constant k_1, k_2	7.9E+15, -1.8
Grain size strengthening constant k, k_3	2374, 0.63
n	1.02
m	0.87
C	0.0067
Melting temperature (°C)	1450
Reference temperature (°C)	27

Our study conducted a comparative analysis of the simulated stresses over the region due to the strain hardening and dislocation strengthening during the MAF. The grain size distribution is also viewed over the region with increased strain imparted after each selected forging pass.

Figure 43 depicts the outcomes of the numerical simulations' predictions for the strain and stress distributions and corresponding contours in the specimen's midplanes and front surface (perpendicular to the constrained direction) for MAF-1, MAF-3, and MAF-5. The simulation results do not accurately replicate the experimental distortions in the shape of the specimens (shown in Fig. 31) during MAF. This discrepancy is likely attributed to the absence of crystallographic texture effects in the simulation. Additionally, the simulation displays an "X"-shaped deformation pattern. According to earlier findings based on microstructural and numerical simulation evaluations of MAF methods, a more considerable strain was observed in the central portions of all specimens [201-202]. After one pass of MAF, the maximum strain in the central region is approximately 0.6, exceeding the external strain value of 0.46. The maximum strain observed in the central region of the specimens following five passes of MAF is approximately 2.6, surpassing the magnitude of the applied external strain value 2.3. The simulations show that the specimen’s central portion, which undergoes more deformation, exhibits a comparatively greater size, as seen by the red contour. This suggests that more passes may be a factor in expanding the severe plastic region of the specimen’s center section.

Figures 43(b-c) compare dislocation generation and the grain size evolution after each pass of MAF as estimated by numerical simulation. Both dislocation generation and grain size distribution predicted here at the corresponding level of equivalent strain (utilizing Eqs. (22) and (23) in VUMAT subroutine) thus offer visual insights into dislocations' evolution and grain size distributions during MAF simulation in 3-D. The accumulation of

dislocations as the strain increases is further supported by the KAM map, as shown in Fig. 36. The grain size distribution exhibits a reverse pattern in relation to dislocation density distribution, with coarser grain size predominantly observed in the outer region and finer grain size in the central part. Additionally, the increasing strain over the course of the five MAF passes is highly correlated with grain size refinement.

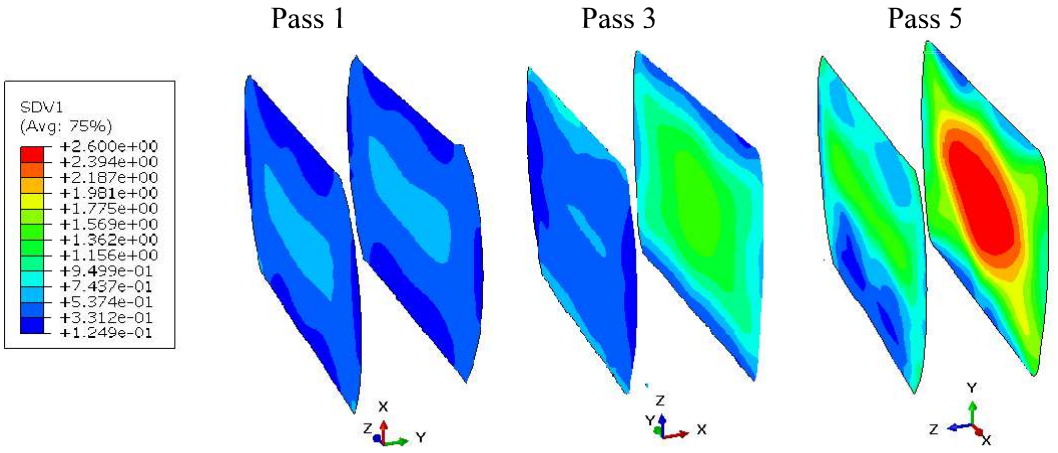

(a)

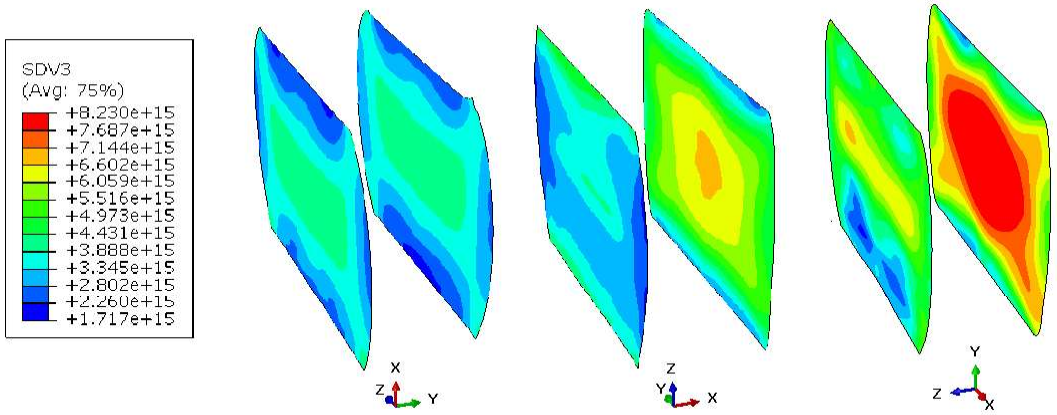

(b)

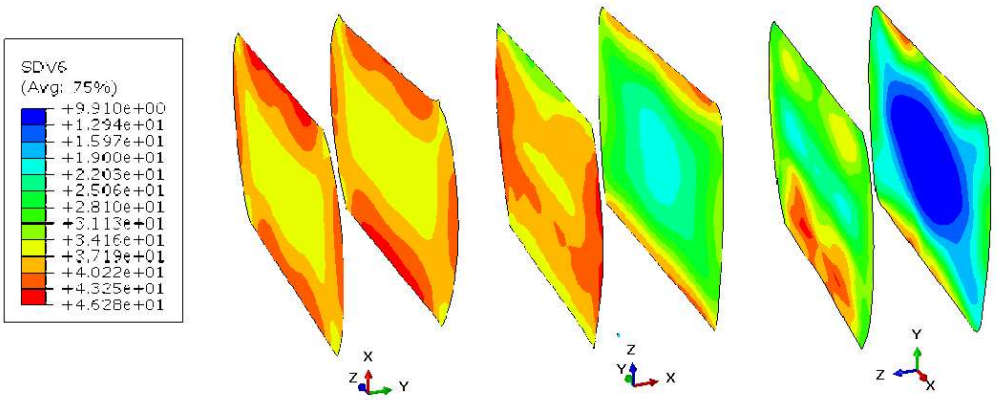

(c)

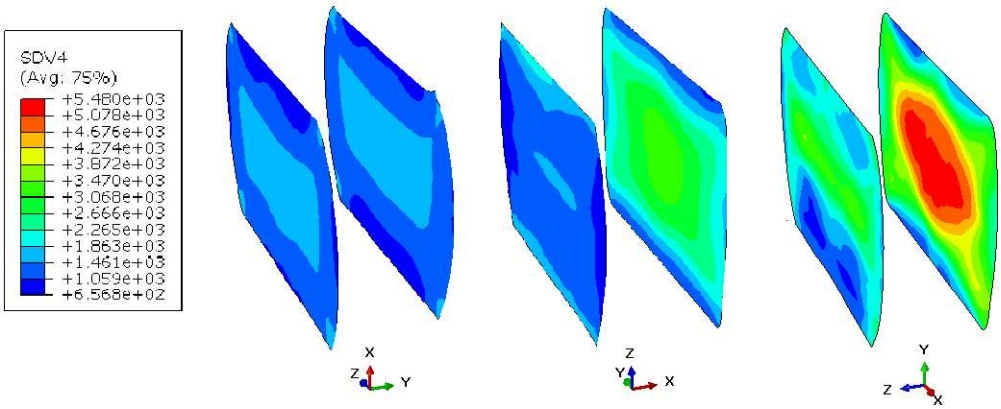

(d)

Fig. 43: Simulation results Simulation results for (a) equivalent strain map, (b) dislocation distribution map (m^{-2}), (c) grain size distribution map (μm) and (d) flow stress map (MPa).

On the other hand, Fig. 43(d) shows a marked rise in stress levels when MAF is performed. The steady rise in strain hardening and dislocation density with increased MAF passes supports the increased stress levels found in this finding. Consistent with previous studies [48], [160], [203], our findings align with the observation of higher stress values following severe deformation. The thermally driven dislocation climb and cross slip mechanisms are partially suppressed at very low temperatures and thereby reduce the dislocation mobility and the annihilation of dislocations at grain boundaries. During MAF pass at lower

temperatures, this combination causes an increase in the equivalent strain as well as an increase in dislocation density.

The predicted dislocation density and grain size at the exact position shown in Fig. 43a after each MAF stage are compared with the corresponding measured results. The primary goal of this study is to correctly forecast the behavior of the Fe-30Mn-9Al-0.8C steel, in particular in the core region under extreme strain. This requires extending the FEA to include the complete body's microstructural evolution based on strain-dependent constitutive relations, as explained in section 7.2.1. The dislocation density is measured from XRD analysis (Fig. 34a) and grain size is measured from the EBSD analysis (Fig. 35e-h). In the modified J-C model (equation 21), the influence of the strain-dependent dislocation density (Eq. (22)) and the grain size (Eq. (23)) parameters has been integrated. Both of these microstructure features contribute to the yield strength after each MAF pass. So, the modified J-C model incorporated with FEA shows good agreement with measured dislocation density and grain size values during MAF-1, MAF-3, and MAF-5 and provides visual confirmation of the progressive build-up of dislocations and grains in response to increasing strain levels. Also, it predicts good yield strength value after each MAF pass. Figure 44 shows the comparison of experimental yield strength values to the simulated yield strength. Initially, up to 3 passes, the FE simulation predicts similar strengthening to yield value. However, after three passes, the predicted value shows a lower deviation from the experimental results. The grain size effect is less in earlier passes of MAF. However, the influence of both dislocation density and grain size reduction is incorporated to compute the flow stress via the material constitutive equation. Additionally, the small number of MAF passes (up to a medium strain level) used in this work is comparable with common cold forging procedures. Furthermore, existing literature supports the notion that in low-strain cold working processes, dislocation density is the main factor for material

strengthening in low-strain cold working methods.[180-181], [203-204]. Grain refinement becomes more prominent in conjunction with the dislocation density for higher strains, particularly after three passes of MAF. At this stage of the MAF process, the cumulative effect of strain leads to a significant increase in dislocation density and grain refinement, highlighting the combined influence of these factors on the material's mechanical properties. This finding emphasizes the importance of considering grain refinement and dislocation density when analyzing the material's behavior at higher strain levels in the MAF process. The simulation study shows that the yield strength of the material depends on depth from the surface of the forged sample (Fig. 45). The strength is maximum at the centre and it decreases towards the surface. There can be a minor error between physical sampling for tensile test and average depth considered for reporting the yield strength from the simulation. In addition, the effect of texture is not considered in the simulation. When the textured material is multiaxially forged, it is expected that the intensity of texture goes down or changes towards randomisation due to multidirectional flow or deformation [51]. The texture material is highly anisotropic whose strength is low in a particular direction. As the material randomises, it becomes isotropic and its strength increases. Therefore, the simulated strength is lower than the experimentally measured value.

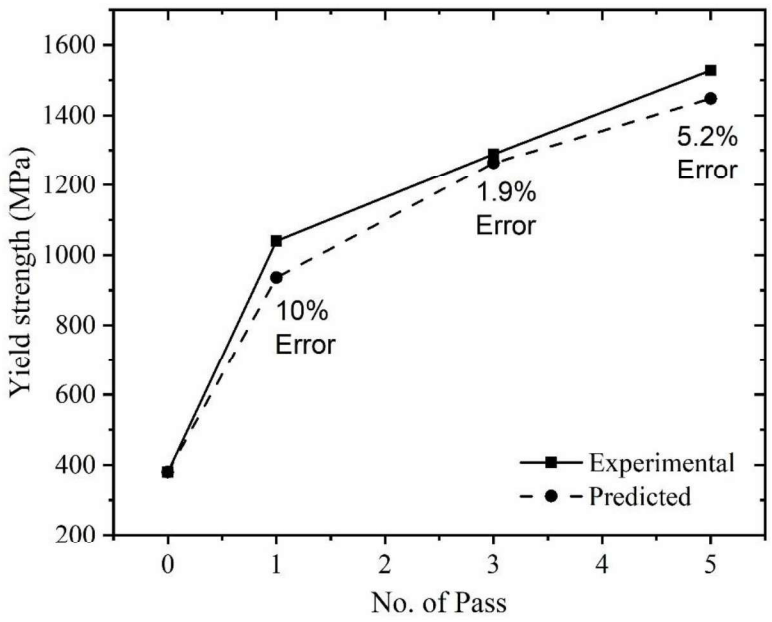

Fig. 44: Prediction of yield strength with respect to experimental results.

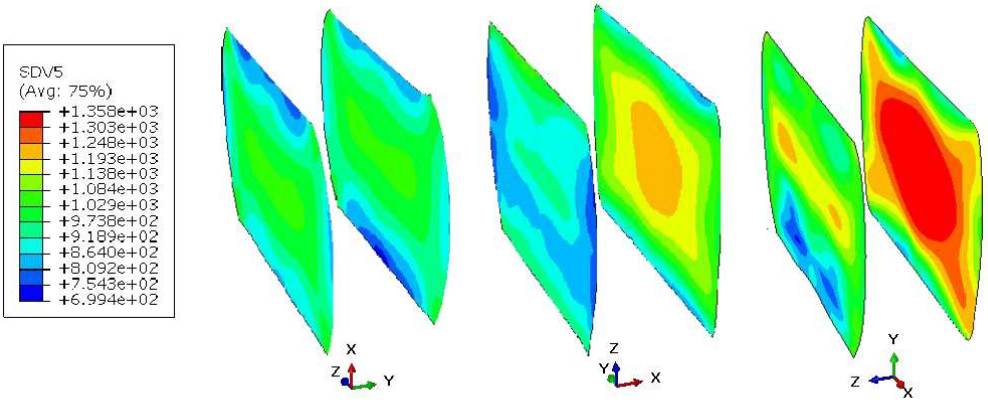

Fig. 45: Simulation results for yield strength map (MPa).

7.1 Conclusions

The objective of the present study is to thoroughly understand and predict the microstructural changes of Fe-30Mn-9Al-0.8C low-density steel during its MAF by FE simulation and their relationships to the material's yield strength. Both experimental as well as FE simulation results have been presented. The main findings of the current investigation therefore are as follows:

- The deformed sample exhibits high dislocation density but low degree of grain refinement. Therefore, the predominant factor contributing to the strengthening of yield strength in the present MAF is the notable increase in dislocation density.
- The FE model of MAF incorporating the modified J-C material model agrees well with the experimental prediction of dislocation density distribution, grain size and yield strength at every pass of MAF., thus the proposed modified J-C model may also be confidently used for other cold deformation processes.
- The yield strength of the material increases from the surface to depth of the forged sample.
- The simulated strength is lower than the experimentally measured value. This may be due to the fact that the material is getting randomised and hardening parameter is changing at higher strain.